Masonry Gravity Dams
A numerical application for stability analysis

BRETAS, EDUARDO M.[1]; LEMOS, JOSÉ V.[2]; LOURENÇO, PAULO B.[3]

ABSTRACT:
This work presents a numerical application for stability analysis of masonry gravity dams. From the geometrical dimensions, the material characteristics, hydrostatic loads and seismic loads, the application automatically determines the following results: thrust line for the dead weight load and the dead weight together with the other loads; stress diagram and safety factors for the failure of the dam-foundation contact as part of an overall analysis; safety factors for the failure of horizontal planes along the body of the dam; parametric properties analysis (volumetric mass) and the resistant characteristics (friction angle) on the base of the dam.

The analyses of three historical masonry dams located in Algeria were made. This work highlights the capacity of the numerical application as it can work with different section geometry, including curved and discontinuous sections, and the importance of assessing several scenarios in the scope of a preliminary and expedite safety evaluation.

Keywords: *Masonry dams, historical structures, numerical applications, stability analysis*

1 HISTORICAL MASONRY DAMS

The first dams built in 3000 B.C. were constructed of earth and rock, laid out randomly. This typology permitted to close wide valleys but only with small height. As in other fields, the Romans gave great contributions to dam construction. Their ability to manage large projects and the introduction of technical improvements, such as the strong hydraulic mortar, are good examples.

The second half of 19th century inaugurates a new era in the dam engineering. The works of Sazilly [1], Delocre [2] and Rankine [3] stated design principles for the dam profile. It was a technological evolution in which the economy of material was much relevant. Figure 1 compares the section of Puentes dam, constructed between 1785 and 1791, in Spain, and Furens dam, completed in 1866 in France, designed by Delocre. Both of the dams present a stable geometry but the volumes differ about 45%. Only after the collapse of Bouzey dam, in 1895, the uplift effect began to be accounted as an important load. Lévy's [4] paper has to be pointed out as the most relevant contribution in this direction.

Masonry by definition has a discontinuous nature. To achieve a homogeneous behaviour, also impervious monolith, different construction techniques were developed. Rankine (1872) described the care that must be taken to ensure that every stone shall be "thoroughly and firmly bedded" and to avoid "the practice of grouting" just for filling voids, which should be filled by stone blocks.

[1] Universidade do Minho, ebretas@lnec.pt
[2] Laboratório Nacional de Engenharia Civil, vlemos@lnec.pt
[3] Universidade do Minho, pbl@civil.uminho.pt

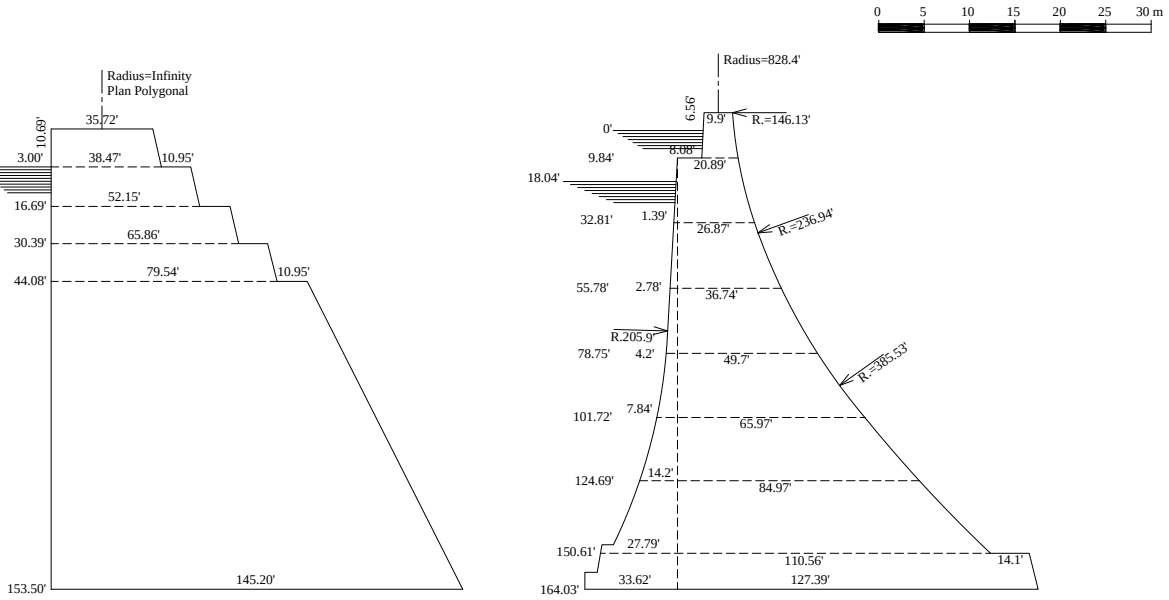

(a) Puentes dam (b) Furens dam

Figure 1. Puentes dam (a) and Furens dam (b) cross sections [after 5]

The masonry applied in the construction of dams may be classified in the following types [6, 7]: dimension stones, rubble masonry and concrete masonry. The dimension stone, regular pieces well shaped, were used for the faces and for ornamental propose, as in the parapet walls and copings. Rubble masonry was the main material, made with irregular stones, as extracted from the quarry, laid in discontinuous layers and bonded with high quality mortar. The concrete masonry, composed by a mix of Portland cement and broken stones, was applied in the foundation and abutments to fill the voids and seams in the bedrock. The size of the pieces assembled in the rubble masonry varies. The largest stones, about 25% of the total aggregates, should be small than 0.75m^3 and the smallest stones, again about 25% of the total aggregates, should has the size that “two men can be handle”, which means probably 50kg [8].

The construction of La Verdeja dam localized near Avila de los Caballeros, in Spain, finished in 1901, according to the above statements. The dam was torn down in 1989 before being submerged by the reservoir of another dam constructed upstream. The core was made by rubble masonry composed by hydraulic lime. Portland cement was employed only close to the joint between ashlars, in the external faces, where extra quality stone was used [9].

In the first quarter of 20th century, rubble masonry has been replaced by concrete masonry to a great extent. This could contain a large percentage of large “plums” to allow cement saving. Aspects like fluidity of the concrete and quality of building joints start to arise [10].

Many of these old masonry dams remain under exploration and safety assessment is an important issue, since the risk is high. Understanding the design assumptions and the construction details underlying their conception helps to evaluate the behaviour and to detect weaknesses. The method presented here is an expedite procedure based on the limit analysis of gravity dams.

2 INITIAL ASSUMPTIONS

It is reasonable that safety evaluation of existing structures begins with expedite procedures. In a first stage, it is important to identify the phenomena under study and the sensitivity of the main variables. Subsequently, through more sophisticated analyses, which require larger resources and therefore must be ascribed to the previously identified scenarios, the early results must be confirmed and the safety factors must be determined.

Figure 2 show the loads involved in gravity dams analysis, namely: self weight W; upstream horizontal ($HP_{h,u}$) and vertical ($HP_{v,u}$) hydrostatic pressures; downstream horizontal ($HP_{h,d}$) and vertical ($HP_{v,d}$) hydrostatic pressures; upstream horizontal ($HPd_{h,u}$) and vertical ($HPd_{v,u}$) hydrodynamic pressures; inertial force of the body of the dam (I_h); and resultant of the uplift at the base between the upstream face and the drainage gallery ($U_{tot,u-g}$) and between the drainage gallery and the downstream face ($U_{tot,g-d}$).

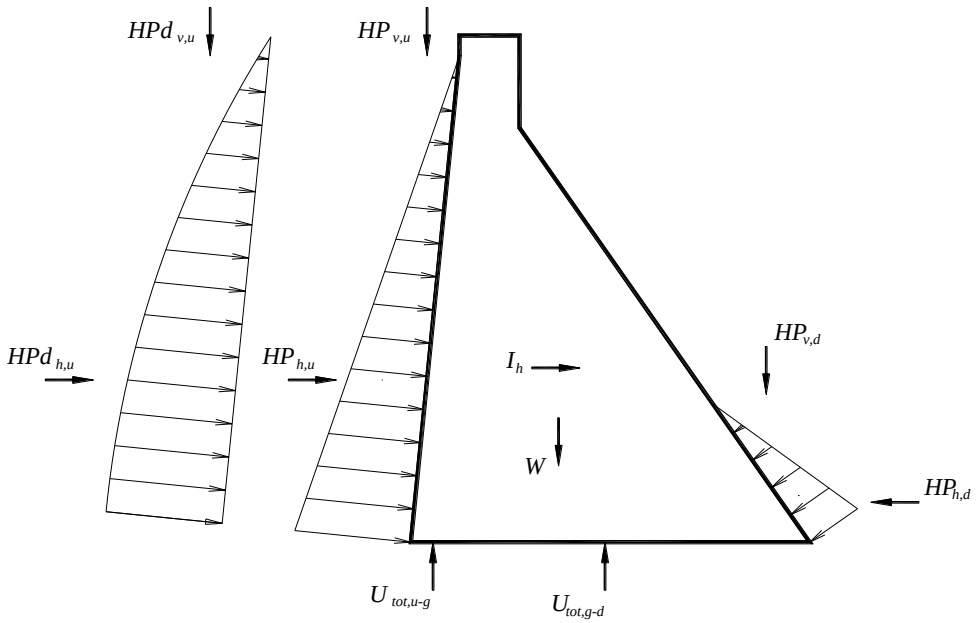

Figure 2. Loads addressed by the numerical application

This is a plane analysis, therefore applicable to straight gravity dams built on wide valleys. For dams presenting a small in plan curvature, the arch effect is disregarded and the results are conservative, so three-dimensional models may be recommended for a more accurate estimate [11, 12].

Furthermore, this method does not take into account the relative deformability of the dam and foundation. This aspect is important for determining the stress values along the base, in the contact between the dam and the foundation, because actual stresses may be higher, especially when the actions are analyzed independently. If the foundation is highly deformable or if it presents a large heterogeneity, such fact cannot be disregarded since it influences the stresses developed on the body of the dam. The compressive stresses installed on a gravity dam are usually fairly low, and below the material strength for concrete and masonry, and the same can be stated for medium strength foundations, which is why, in a expedite calculation, compressive failure is not considered. This is why the concrete dams use low strength or pozzolanic cements, for economic and practical reasons, because these cements have lower hydration temperatures than the ones with high strength. On the other hand, the tensile strength is considered null, which relevant for the determination of the length of cracks occurring at the base, as well as for the application of the uplift by an iterative procedure.

A Mohr-Coulomb failure model, with null cohesion, was adopted for the horizontal plane. Therefore, the friction angle is the only shear strength parameter considered. This is justified by the fact that cohesion is difficult to determine by experimental means and has a large scatter. Hence, most international regulations require the use of high partial safety factors, or to disregard it completely. In addition, cohesion only acts in practice when the section is under a minimum compressive stress, so if this aspect is not observed, it would be unsafe to consider it throughout the

entire length of the plane under analysis [13]. Uplift is not considered as an external load, which is why it is not included in the free body diagram. Uplift is locally added to the total vertical stress to obtain effective stresses. If the foundation has a drainage system, the uplift is reduced, leading to a bi-linear uplift diagram, depending on the location of the gallery. A pseudo-static seismic analysis method is adopted, considering the inertial force of the dam and the hydrodynamic effect of water in accordance with Westergaard's solution. It is a simplified method that does not consider the amplification of the value of earthquake acceleration in height and its oscillatory characteristic, being the resultants applied as static loads.

3 NUMERICAL DATA FOR THE MODEL

The calculations are done on a model developed from the idealization of a discrete medium consisting of horizontal elements (Figure 3), which are geometrically represented by the corresponding axes, and defined by the intersections between planes, with upstream and downstream faces. The element thickness (e) may be chosen depending on the dam height. From several analysis done, values of $e = 0.10m$ have been adopted for dams up to 30m height and of $e = 0.50m$ for larger heights.

The required data for the element are: length (L^n); abscissa of the centre (x_c^n); level of the axis (y^n); and abscissa close to the upstream (x_u^n) and downstream (x_d^n) face. Three parameters can be considered independent (x_u^n, x_d^n, y^n), being the remaining ones introduced to optimize the calculations, with the following relations:

– Length of the element

$$L^n = x_d^n - x_u^n \tag{1}$$

– Abscissa of the centre of the element

$$x_c^n = \frac{x_u^n + x_d^n}{2} \tag{2}$$

The loads presented in Figure 2 are considered, at the level of element n, as follows (Figure 4):

– Self weight

$$W^n = L^n e \gamma^{mat} \tag{3}$$

– Upstream horizontal hydrostatic pressure

$$HP_{h,u}^n = \left(z_{HP,u} - y^n\right)\gamma^w e \Leftrightarrow z_{HP,u} \geq y^n \tag{4}$$

– Upstream vertical hydrostatic pressure

$$HP_{v,u}^n = \left(z_{HP,u} - y^n\right)\gamma^w \left(x_u^n - x_u^{n+1}\right) \Leftrightarrow z_{HP,u} \geq y^n \tag{5}$$

– Downstream horizontal hydrostatic pressure

$$HP_{h,d}^n = \left(z_{HP,d} - y^n\right)\gamma^w e \Leftrightarrow z_{HP,d} \geq y^n \tag{6}$$

– Downstream vertical hydrostatic pressure

$$HP_{v,d}^n = \left(z_{HP,d} - y^n\right)\gamma^w \left(x_d^{n+1} - x_d^n\right) \Leftrightarrow z_{HP,d} \geq y^n \tag{7}$$

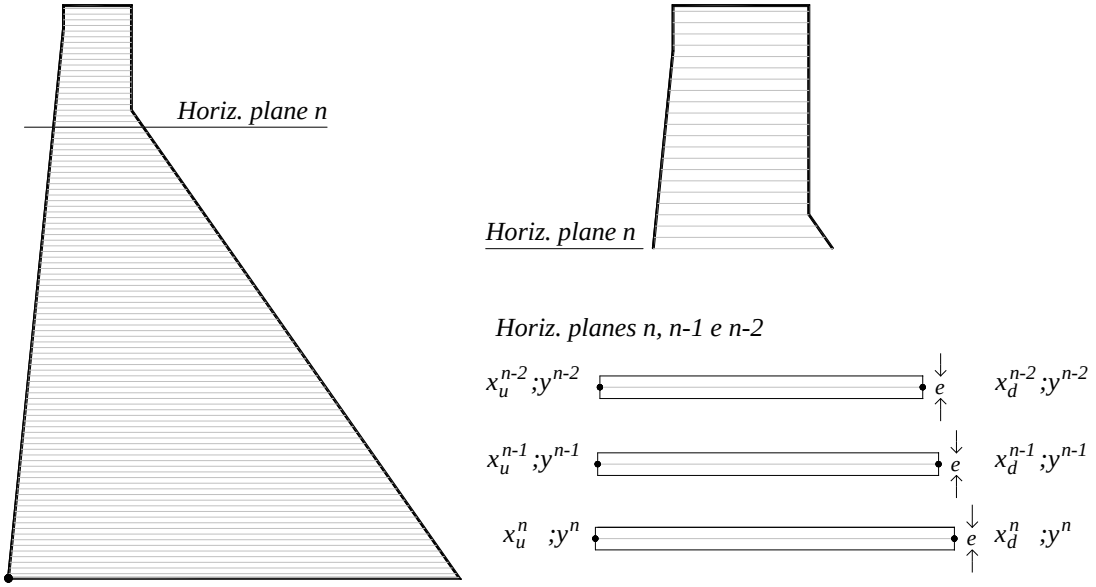

Figure 3. Discretization scheme of the dam body

– Upstream horizontal hydrodynamic pressure (Westergaard's solution)

$$HP_{h,u}^n = \frac{7}{8} a_h \gamma^w \sqrt{\left(z_{HP,u} - y_{found}\right)\left(z_{HP,u} - y^n\right)}\, e \Leftrightarrow z_{HP,u} \geq y^n \tag{8}$$

– Upstream vertical hydrodynamic pressure

$$HP_{v,u}^n = \frac{7}{8} a_h \gamma^w \sqrt{\left(z_{HP,u} - y_{found}\right)\left(z_{HP,u} - y^n\right)}\left(x_u^n - x_u^{n+1}\right) \Leftrightarrow z_{HP,u} \geq y^n \tag{9}$$

– Inertial load

$$I_h^n = L_n e \gamma^{mat} a_h \tag{10}$$

Here, γ^{mat} is the volumetric weight of the material, γ^w is the volumetric weight of water, $z_{HP,u}$ is the upstream water level, $z_{HP,d}$ is the downstream water level, y_{found} is the foundation level and a_h is the seismic coefficient in the horizontal direction

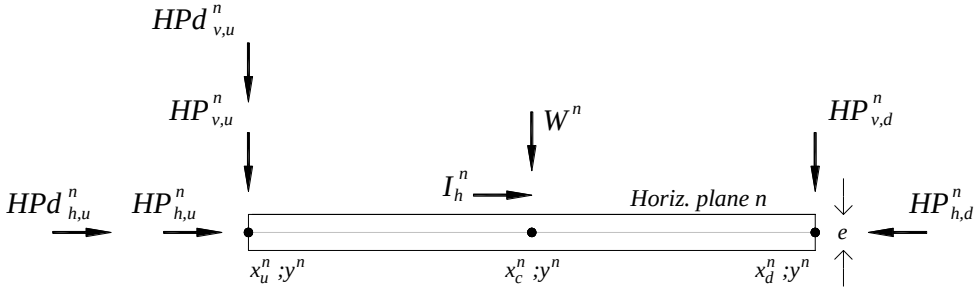

Figure 4. Load representation in single element

The hydrostatic and the hydrodynamic pressures acting on the face of an element are assumed with a rectangular distribution, which is an acceptable approximation for small thickness elements (e).

For a given horizontal plane, the analysis is done from the integration of the thickness elements (e) placed above such plane. The smaller the discretization thickness adopted, the higher the accuracy of results, i.e., by taking the self weight as an as example, the following holds:

$$\lim_{e\to 0}\left|\sum W^n - W\right| \to 0 \tag{11}$$

4 DETERMINATION OF RESULTS

The application makes it possible to visualize on a graph the thrust lines due to the action of self weight, corresponding to the situation of empty reservoir, and to the combined action of self weight with other actions. The concept of thrust line results from the graphic statics and corresponds to the geometrical place occupied by the static resultant in each horizontal plane of loads applied above that plane. It has an important physical meaning, because it represents the load distribution across the body of the structure. Through its observation, it is possible to identify tensile zones, which is the case of the planes in which the thrust line is outside the middle third of the section. Furthermore, it is also possible to observe on a graph the diagram of total and effective vertical stresses. The total stresses are obtained in the following way:

$$\sigma = \frac{\sum V}{A} \pm \frac{\sum M}{I} y\,, \tag{12}$$

in which,

σ – Total vertical stress;

$\sum V$ – Sum of the vertical component of actions (except for uplift, which was not considered as an external action);

$\sum M$ – Sum of moments due to actions;

A – Area of the base (per meter of the dam length);

I – Inertial moment of the plane (per meter of the dam length);

y – Distance to the downstream and upstream faces.

The effective stresses are determined from total stresses by adding the uplift pressure. Generally, the uplift diagram presents a bi-linear configuration (Figure 5a), resulting from the triangular diagram and from the effect of the reduction in the drainage system. The diagram can be updated whenever a new crack arises, close to the upstream face, where the full uplift is applied (Figure 5b) [14], leading to the iterative calculation of the final length of the crack. The initial length of the crack, for a previously defined load scenario, is determined on the basis of the criterion of null tensile resistance. The calculation of the final length of the crack takes into account the assumptions as follows:

- After the occurrence of the initial crack, it is considered that the drainage system looses its effectiveness (other less conservative hypotheses would be admissible, such as considering the loss of effectiveness of the drainage system only in the cases when the crack was developed beyond the zone of installation of the drains), and, therefore, the pressure diagram acquires a rectangular configuration along the crack and a trapezoidal or triangular configuration, depending on the downstream water level, along the non-cracked surface;
- Unlike the previously adopted strategy, the uplift becomes part of the eccentricity and stress calculations; otherwise it would not be possible to establish an iterative calculation method to simulate the progression of the crack.

The factor of safety to sliding (SSF), in any horizontal plane, including the base, for the actions applied above their level, is given by:

$$SSF = \frac{\left(\sum V\right)\tan\phi}{\sum H}\,, \tag{13}$$

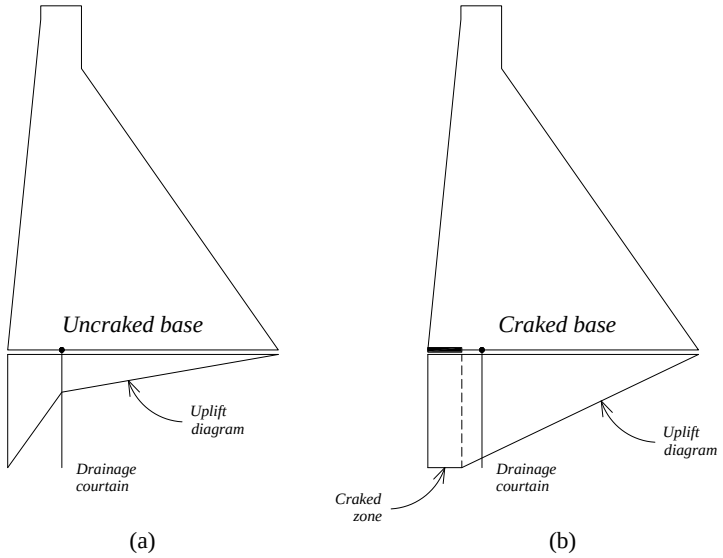

Figure 5. Uplift diagram for uncracked base (a) and cracked base (b)

in which $\sum V$ is the sum of the vertical component of actions (including the uplift. In this case, the effect of uplift can be physically interpreted as a reduction factor in self weight [15]), $\tan\phi$ is the tangent of the friction angle and $\sum H$ is the sum of the horizontal component of actions.

The overturning safety factor (OSF) is given by:

$$OSF = \frac{\sum M_{sta}}{\sum M_{ope}},$$

in which $\sum M_{sta}$ is the sum of stabilizing moments and $\sum M_{ope}$ is the sum of acting moments.

For the analysis throughout the body of the dam, in the various horizontal planes defined from the thickness (e), the full uplift is considered for these levels, without any reduction factor, because it is assumed that there is no vertical drainage system installed on the body of the dam. The other actions reflect the load cases adopted.

The available parametric analysis, for the self weight and the friction angle, refer to the horizontal plane of contact between the dam and the foundation and to the load cases considered, according to the hypotheses admitted for the uplift.

5 THREE MASONRY DAMS IN ALGERIA

In the end of the 19th century the French government was involved in the construction of several masonry dams in Algeria for irrigation and water supply. Three of them, Gran Cheurfas (Figure 6a), 39.9m of height, finished in 1884 and failure in 1885, Habra (Figure 6b) , 38.1m of height, finished in 1871 and failure in 1881, and Hamiz dam (Figure 6c) , 38.1m of height, finished in 1885, are worthy of special attention since they collapsed. In fact, they were designed before Bouzey dam accident and were not prepared to withstand the uplift pressure. As in other examples this aspect plays a key role in dam behaviour and the collapse mechanism.

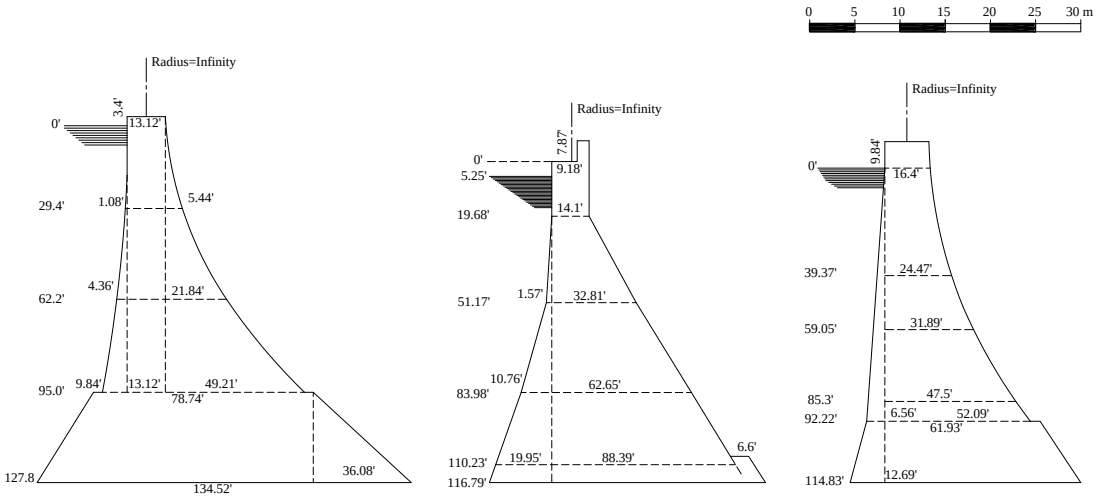

(a) Gran Cheurfas dam (b) Habra dam (c) Hamiz dam

Figure 6. Cross sections of Gran Cheurfas (a), Habra (b) and Hamiz (c) dam [after 5]

In the case of Gran Cheurfas dam and Hamiz dam information about the collapse is limited. Based on the analyses developed for Gran Cheurfas dam (Figure 7) and Hamiz dam (Figure 8), it is possible to conclude that collapses were triggered by crack propagation near the foundation, followed by an uplift increase. The rupture of Habra dam is more documented since it cost 209 lives. According to Smith [16], Habra collapsed could have been predicted if the technical and scientific community had paid attention to the Bouzey accident. Wegmann [6] described that Habra dam ruptured after an "unusually severe storm" when "forming a large wave whose height can be calculates about 1m". Figure 9 plots the results for the two following conditions: operating level (OL) and flood level (FL). For flood level, crack development process was computed with initial length of 9.7m (tensile stress zone). With no tensile strength and full uplift upgrade scheme, the section is not stable.

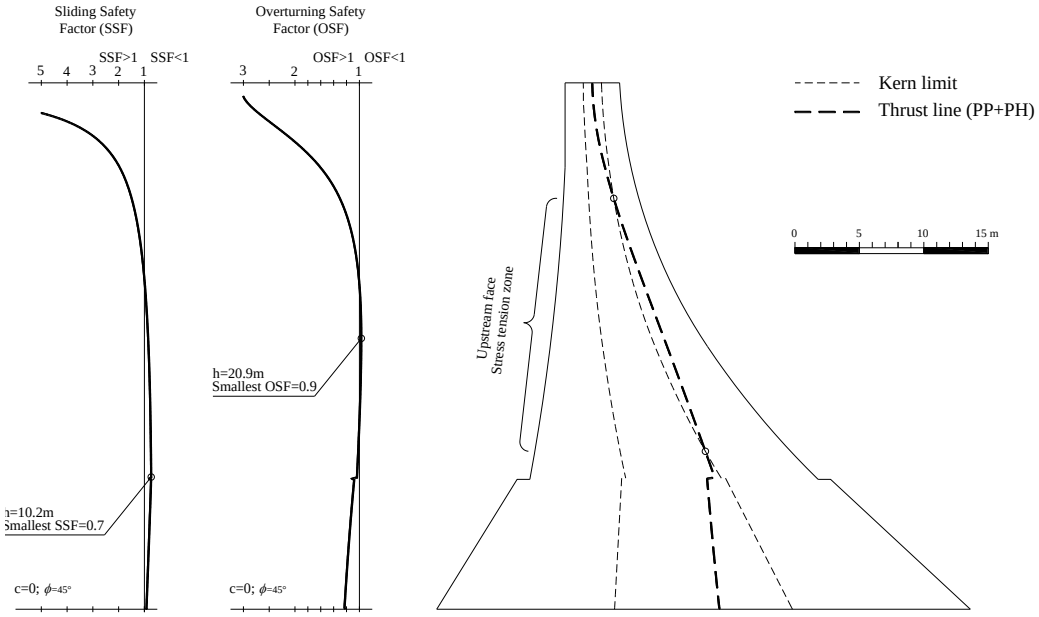

Figure 7. Gran Cheurfas dam analysis

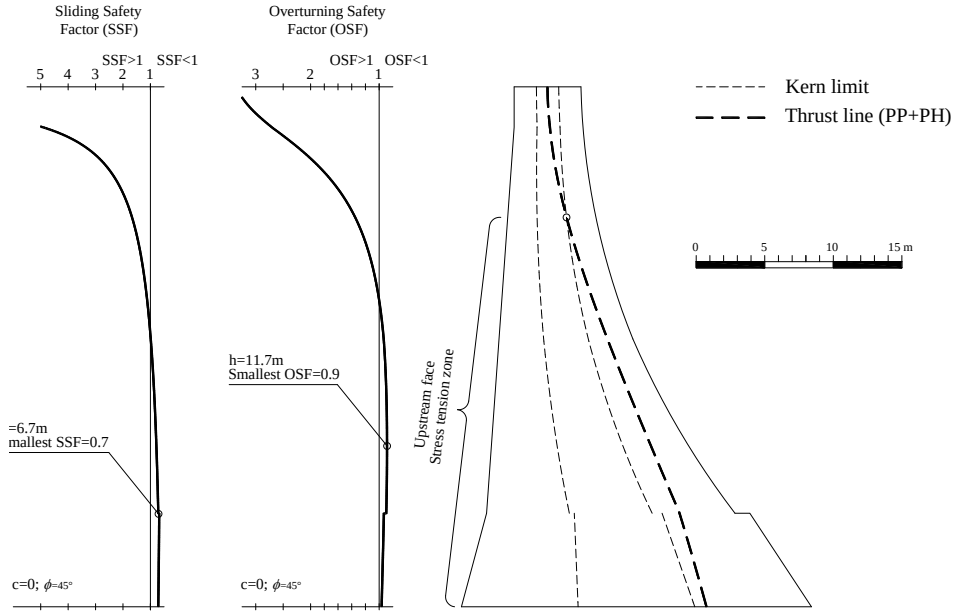

Figure 8. Hamiz dam analysis

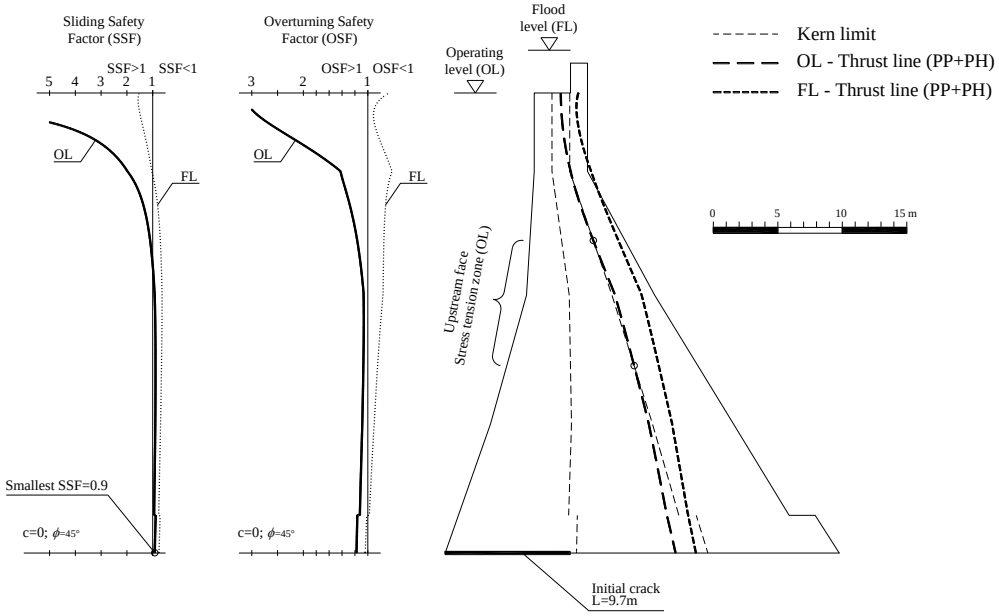

Figure 9. Habra dam analysis

6 CONCLUSIONS

An application developed for the expedite assessment of the safety conditions of gravity dams was presented. It has much flexibility, as profiles of different geometry, including curved faces and discontinuities, can be studied. Several examples of such profiles have been presented.

From the results computed for the case studies, dams for which uplift was not considered in their design are likely not to satisfy the safety conditions prescribed by current regulations. In many cases, this fact motivated the execution of rehabilitation works and three collapses in Algeria were discussed.

ACKNOWLEDGEMENTS

This work has been funded by FCT (Portuguese Foundation for Science and Technology) through the PhD grant SFRH/BD/43585/2008, for which the first author is grateful.

REFERENCES

[1] Sazilly, J., *Note sur un type de profil d'égale résistance proposé pour les murs de réservoirs d'eau.* Annales des Ponts et Chassées, 1853. **6**: p. 191-222.

[2] Delocre, F., *Mémoire sur la forme du profil à adopter pour les grands barrages en maçonnerie des réservoirs.* Annales des Ponts et Chassées, 1866.

[3] Rankine, W.J.M., *Miscellaneous scientific papers: Report on the design and construction of masonry dams*. 1881, London: Charles Griffin and Company.

[4] Lévy, M.M., *Quelques considérations sur la construction de grands barrages.* Comptes-Rendus de l'Académie des Sciences, 1895. **6**: p. 288-300.

[5] Morrison, C.E. and O.L. Brodie, *Masonry dam design, including high masonry dams*. Second Edition ed. 1916, New York: John Wiley & Sons, Inc.

[6] Wegmann, E., *The desing and construction of dams*. 1899, New York: John Wiley & Sons.

[7] Courtney, C.F., *Masonry dams, from inspection to completion*. 1897, London: Crosby Lockwood and Son.

[8] Pionner Electric Power Co., *Masonry dam and spillway*. 1896, Ogden, Utah: Hestmark & Wilcox, Printers and Binders.

[9] Caballero, M.R.C., I.L. Martín, and M.G. Martín, *La presa de La Verdeja. Una presa representativa de principios de siglo rescatada de las aguas del embalse del Castro de las Cogotas*, in *I Congreso de Historia de Las Presas*. 2000: Mérida, España.

[10] Creager, W.P., *Engineering for masonry dams*. 1917, New York: John Wiley & Sons, Inc.

[11] Herzog, M.A.M., *Spatial action of straight gravity dams in narrow valleys.* Journal of Structural Engineering, 1989. **115**: p. 698-706.

[12] Lombardi, G., *3-D analysis of gravity dams.* Hydropower & Dams, 2007(One): p. 98-102.

[13] Leclerc, M., P. Léger, and R. Tinawi, *Computer aided stability analysis of gravity dams - CADAM.* Advances in Engineering Software, 2003: p. 403-420.

[14] USACE, *Evaluation and comparison of stability analysis and uplift criteria for concrete gravity dams by three Federal Agencies*. 2000: Washington, D.C.

[15] Serafim, J.L., *Influence of Interstitial Water on the Behavior of Rock Masses*, in *Rock Mechanics in Engineering Practice*, K.G. Stagg and O.C. Zienkiewicz, Editors. 1968, John Wiley & Sons: London. p. 55-92.

[16] Smith, N., *A history of dams*. 1971, London: Peter Davies.